# Designing a Permanent Magnet Linear Generator Multi Air-gap Structure using the Finite Element Method.

Pierre Kenfack, Daniel Matt, and Philippe Enrici

Institute of Electronics and Systems, University Montpellier, CC05001-860 rue Saint Priest, 34095 Montpellier cedex 5, France
(e-mail: first-name.name@ies.univ-montp2.fr).

## Abstract

**This paper deals with the design of a Permanent Magnet Linear Generator Multi Air-gap Structure (MALG) using the Finite Element Method (FEM). The cogging force, which occurs due to the interaction between stator teeth and the Permanent Magnet (PM), is reduced by the MALG dimensions. The generated voltage is analyzed for both no-load on the multi-air gap flux density. This paper predicts the thrust force and flux linkage.**

## 1. Introduction

Linear electric machines are electromagnetic, electrostatic, piezoelectric, and magneto-striction force devices capable of producing progressive or oscillatory translational (linear) motion directly [1, 2, 3].

A Permanent Magnet Linear Generator Multi Air-gap Structure is an electromagnetic device that develops short travel linear motion. The MALG is intended for an electroacoustic converter. An electroacoustic machine converts acoustic energy into electrical energy, and vice versa, converts electric energy into acoustic energy Fig 1. An acoustic wave is created as "input" using a linear motor. This acoustic wave is amplified by the heat recovered as "output" using a linear generator. The advantages of the Permanent Magnet Linear Generator Multi Air-gap Structure over a traditional structure are its compactness, very high dynamic range due to the lightness of the moving part, and higher efficiency.

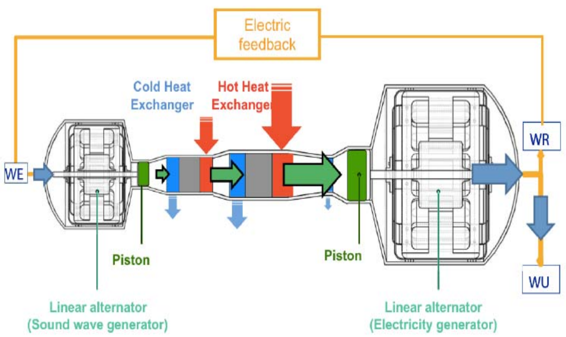


Fig. 1.Electroacoustic converter.

In the multi-air gap concept, the aim is to increase, within a given volume, the number of air-gap surfaces generating electromagnetic conversion [4, 5].

Despite these advantages, the Permanent Magnet Linear Generator Multi Air-gap Structure generally has to deal with a high cogging force. The double-sided linear electric generator has a cogging force that is much lower compared to the single and double-sided iron core generator.

The cogging force is produced by the interaction between the permanent magnet and the slotted iron structure. The cogging force produces a pulsating force ripple resulting in vibrations and acoustic noise that is detrimental to the MALG Structure. This paper presents investigations on methods to reduce cogging force.

In this paper, a MALG Structure is designed using a 2D finite element method. The main design parameters are the electromagnetic force (emf) across the stator bars and the cogging force. The slot opening width length is chosen to give a minimum cogging force. The permanent magnet thickness was varied over a wide range and the voltage and cogging force are calculated each time by FEM.

Fig 2 shows the structure chosen to implement the linear electric generator using 2D FEM ANSYS Maxwell software.

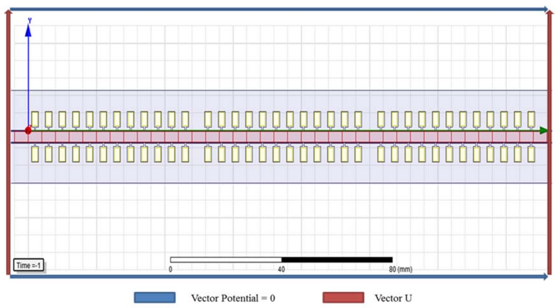


Fig.2 Magnetic structure, three-phase linear generator.

## 2. Calculating main parameters

The first step in designing and analyzing a Permanent Magnet Linear Generator Multi Air-gap Structure is to determine the air-gap field produced by the magnets. The fields may be determined precisely by finite element analysis. Generally, harmonic displacement is used to describe the oscillatory motion of an electric machine or moving part.

### 2.1. Electromagnetic equations

Whereas fields may be determined precisely by finite element analysis, a magnetic circuit approach yields approximate results that are acceptable for practical purposes. Thus, neglecting saturation and leakage, we have:

$$B_m = B_g = \mu_0 * H_g \quad (1)$$

Neglecting the reluctance of core, Ampere's law yields:

$$2gH_g + H_m h_m = 0 \quad (2)$$

Assuming rare-earth magnets, their demagnetization characteristic can be written:

$$B_m = B_r + \mu_{rc} H_m \quad (3)$$

Combining (1), (2) through (3) yields.

$$B_m = B_r \left[ 1 + \frac{\mu_{rc}}{\mu_0} \left( \frac{2g}{h_m} \right) \right]^{-1} \quad (4)$$

$B_m$ : PM operation flux density, T

$H_m$ : PM operation field intensity, A/m

$g$ : Air-gap, mm

$B_r$ : Residual flux density, T

$\mu_{rc}$ : PM recoil permeability, H/m

$B_g$ : Air gap flux density, T

$H_g$ : Air gap magnet field intensity, A/m

$h_m$ : Magnet thickness, mm

The electromagnetic force (emf) is proportional to linear speed.

$$e = -k\dot{x} \quad (5)$$

$e$ : emf, V; $k$ : function with PM flux density and generator width; $\dot{x}$ : speed.

## 2.2. Mechanical equations

The obtained mechanical values prohibit the use of traditional mechanical systems because acceleration is too high.

Displacement of the moving part is written in the following form:

$$x = x_m \sin(2\pi f t); x_m = \frac{L_s}{2} \quad (6)$$

Speed is the derivative of displacement

$$\dot{x} = \frac{L_s}{2} 2\pi f \cos(2\pi f t) \quad (7)$$

Acceleration is the derivative of speed.

$$\ddot{x} = -(2\pi f)^2 * x \quad (8)$$

The speed of synchronism ( $V$ ) or displacement is independent of the number of the permanent magnets pole pairs.

$$V = 2\tau f \quad (9)$$

$L_s$ : the stroke; $f$ : the mechanical frequency and $\tau$ : the pole pitch.

The electromagnetic force is calculated as follows:

$$F(t) = \frac{e(t)\, i(t)}{\dot{x}(t)} \quad (10)$$

The highest interaction electromagnetic force per given current occurs when e(t) and i(t) are in phase with each other.

## 3. Carried out simulations

The main characteristics of the MALG being studied were obtained as in [6, 7, 8].

For our purposes here, ANSYS-Maxwell software was used with the Finite Element Method. Maxwell Transient is able to evaluate interactions between transient electromagnetic fields and motion [9, 10, 11].

The MALG Structure has equal slot and pole pitches. The cross section of the linear electric generator is shown in Fig 3 and specification design data is given in Table 1.

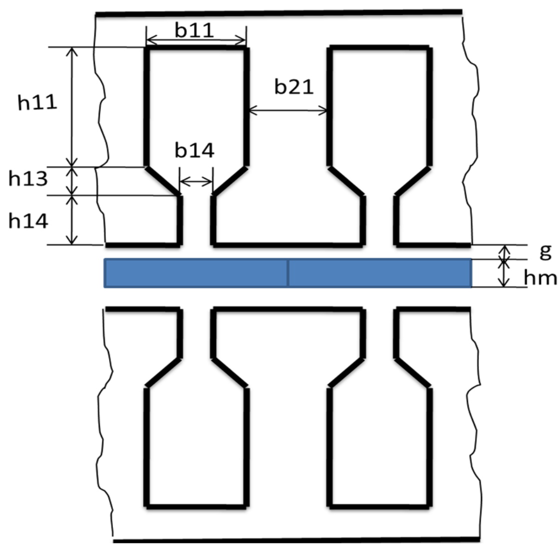


Fig. 3 MALG slot dimensions.

The main variable dimensions are optimized to minimize the cogging force value. The studied variables are the air-gap thickness, PM thickness and slot opening width.

The slot pitch of the structure is:

$$\tau_s = b_{11} + b_{21} \quad (11)$$

$\tau_s$: slot pitch, $b_{11}$: width of rectangular slot, $b_{21}$: width of tooth.

**TABLE 1:** SLOT DIMENSIONS

| Element | Symbol | Value (mm) |
|---|---|---|
| Slot opening height | $h_{14}$ | 1.0 |
| Slot wedge height | $h_{13}$ | 0.0 |
| Slot body height | $h_{11}$ | 5.0 |
| Slot opening width | $b_{14}$ | 0.8 |
| Slot wedge width | $b_{11}$ | 2.0 |
| Slot body bottom width | $b_{21}$ | 2.0 |
| Slot pitch | - | 5.0 |
| Pole pitch | $\tau$ | 5.0 |
| PM length | - | 5.0 |
| PM thickness | hm | 5.0 |
| Air gap | g | 0.8 |
| Generator length | - | 230 |
| Generator width | - | 50 |
| Stroke | Ls | 20 |
| Generator power | 1 kW | |

The slot factor bs and bw are used to draw the cogging force curve with the position, permanent magnet thickness, and air-gap thickness.

bs $= \frac{\text{slot opening width}}{\text{slot width}}$ This parameter gives information on the evolution of the cogging force ([0.20, 0.80]).

bw $= \frac{\text{slot width}}{\text{slot pitch}}$ This parameter gives information on the optimization of winding and the decrease of iron mass ([0.40, 0.60]). Slot width is varied to optimize the bars dimensions.

### 3.1. Air-gap

In the design parameters of the MALG, air-gap thickness is the parameter that has the most influence on performance. The air-gap is very important in the electromagnetic parameterization of a linear generator, because it affects performance.

When the airgap thickness increases, the air-gap magnetic flux density decreases similarly. This helps decrease the cogging force greatly.

We analyzed the cogging force amplitude characteristic with different air-gap thicknesses. The cogging force amplitude characteristic with different air-gap thicknesses and positions is shown in Fig 4.

The maximum flux density in the teeth is 1.3789 T.

### 3.2. PM thickness

We chose NdFeB to make our prototype, with magnetic properties provided in Table 2.

The PM volume is varied with different PM thicknesses and using simulation calculation. Decreasing PM thickness causes a reduction in the equivalent current density of the PM that results in decreasing the cogging force. Reducing PM thickness has more effects, the largest of which is enhancing the linear electric generator output voltage. The moving plate generates varying flux and induces voltage in the windings. The cogging force amplitude characteristic with different permanent magnet thicknesses and positions is shown in Fig 5.

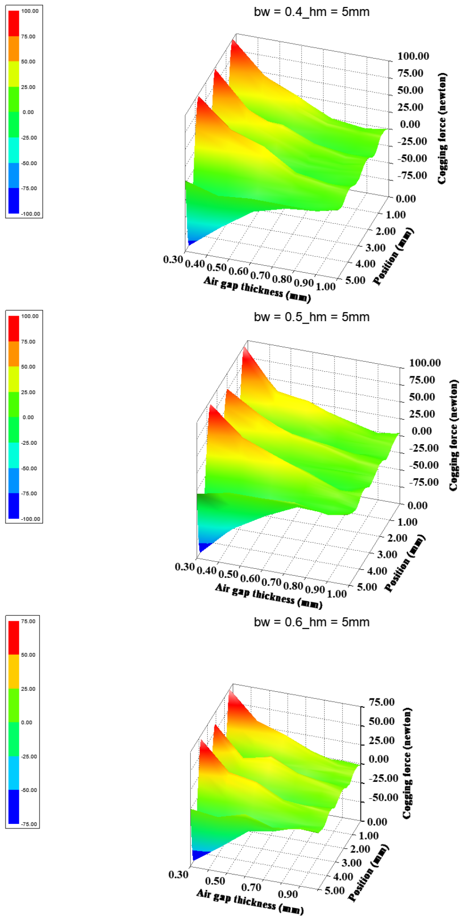


Fig. 4 Cogging force versus position and air-gap thickness.

**TABLE 2:** MAGNETIC PROPERTIES OF MAGNETS

| Characteristic | Units | Min | Nominal | Max |
|---|---|---|---|---|
| **Br**, Residual Induction | mT | 1170 | 1200 | 1230 |
| **HcB**, Coercivity | kA/m | 836 | 887 | 939 |
| **HcJ**, Intrinsic Coercivity | kA/m | 2,388 | - | - |
| **BHmax**, Maximum Energy Product | kJ/m$^3$ | 263 | 279 | 295 |

### 3.3. Slot opening width

We chose to use M300–35A to make our prototype, with typical provided in Table 3. The magnetic properties of a ferromagnetic material are described graphically in terms of the material's **B-H** curves and core losses.

When the slot opening width varies, the flux linking the bars changes as the permanent magnet passes through the slot, affecting the cogging force and output voltage. The semi-open slots in the fixed part can decrease the cogging force, because the cogging force is the interaction between the permanent magnet edges and fixed part slot edges.

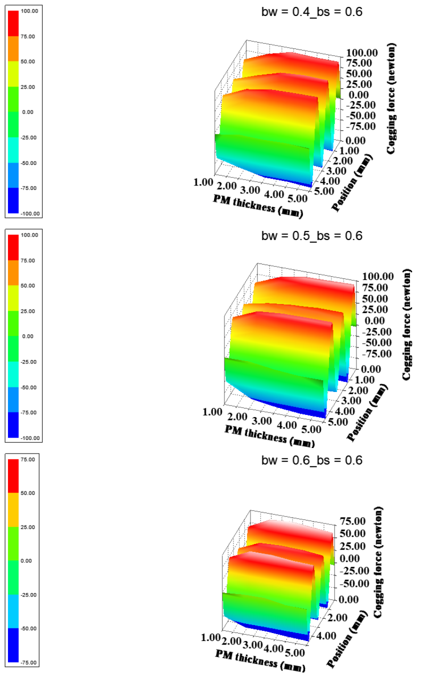


Fig. 5 Cogging force versus position and PM thickness.

**TABLE 3:** TYPICAL DATA FOR M300-35A

| B(T) | H(A/m) at 50 Hz | P(W/kg) at 50 Hz |
|---|---|---|
| 0.1 | 30.9 | 0.03 |
| 0.2 | 40.2 | 0.08 |
| 0.3 | 46.4 | 0.15 |
| 0.4 | 52.1 | 0.24 |
| 0.5 | 57.9 | 0.35 |
| 0.6 | 64.4 | 0.48 |
| 0.7 | 72.0 | 0.61 |
| 0.8 | 81.1 | 0.76 |
| 0.9 | 92.6 | 0.92 |
| 1.0 | 108 | 1.10 |
| 1.1 | 130 | 1.30 |
| 1.2 | 168 | 1.54 |
| 1.3 | 250 | 1.82 |
| 1.4 | 510 | 2.20 |
| 1.5 | 1440 | 2.62 |
| 1.6 | 3490 | 2.98 |
| 1.7 | 6700 | 3.25 |
| 1.8 | 11300 | 3.41 |

Despite a very marked decrease of the cogging force in the case of semi-open slots, the leakage flux is higher, which can reduce the efficiency of the linear electric generator.
The cogging force increases when the relative opening width slot (bs) increases Fig 6.

### 3.4. Optimization

The 2D finite element method is sufficient to analyze the Permanent Magnet Linear Generator Multi Air-gap Structure.

Optimization methods try to find the maximum or minimum of a function where restrictions or constraints on the independent variables may exist.

In optimizing the MALG, the objective function and constraints can be computed using a numerical field computation approach (FEM).

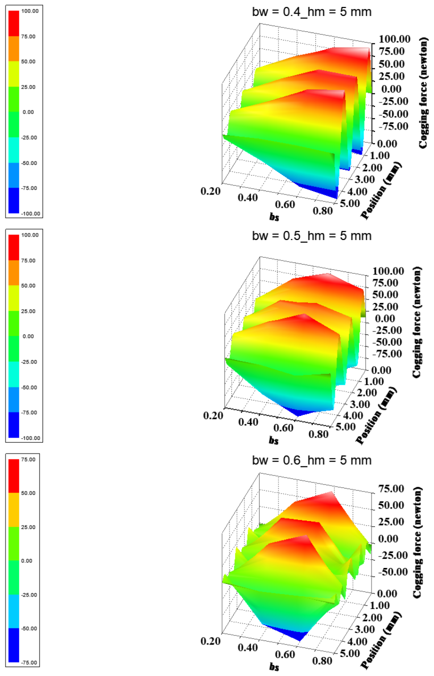


Fig. 6 Cogging force versus position and bs.

MALG optimization can be formulated as a constrained optimization problem with more than one objective (minimization of cost, minimization of the amount of PM material, maximization of efficiency and output power).

The independent variables used in MALG design dimensions are the PM thickness (hm), air-gap (g), relative slot opening width (bs), and relative slot width (bw).

The objective function is not easily expressed in terms of the independent variables. We therefore did use the objective function for modeling directly, but rather for modelling the performance characteristics of the MALG, used in the constraints, in terms of the independent variables. Table 4 shows the final optimized MALG details, with resistive losses using FEM, 70 W (aluminum materials).

The cogging force amplitude is zero in average value per unit area air-gap Fig 7.

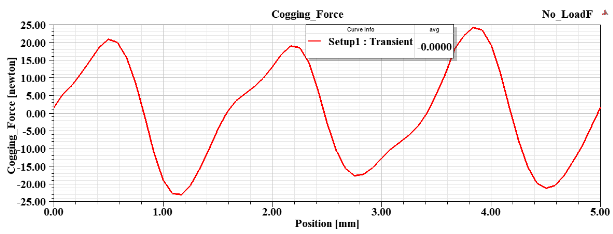


Fig. 7 Cogging force three-phase MALG versus position.

The parasitic contact force between stators and the moving part depends on the air-gap.

At position g = 0.3 mm, the plate is moved laterally. Plate movement increases the area of the lower stator, and decreases the area of the upper stator by an equal amount. The cogging force through the two stators is still equal.

Cogging force is strictly linked to the mutual position of all permanent magnets and all winding.

**TABLE 4:** MALG OPTIMIZATION

| Element | Symbol | Value (mm) |
|---|---|---|
| Slot opening height | $h_{14}$ | 1.0 |
| Slot wedge height | $h_{13}$ | 0.0 |
| Slot body height | $h_{11}$ | 5.0 |
| Slot opening width | $b_{14}$ | 0.5 |
| Slot wedge width | $b_{11}$ | 2.5 |
| Slot body bottom width | $b_{21}$ | 2.5 |
| Slot pitch | - | 5.0 |
| Pole pitch | $\tau$ | 5.0 |
| PM length | - | 5.0 |
| PM thickness | hm | 3.0 |
| Air gap | g | 0.3 |
| Relative slot opening | bs | 0.20 |
| Relative slot width | bw | 0.50 |
| Generator length | | 230 |
| Generator width | | 50 |
| Stroke | Ls | 20 |
| PM mass | 0.25875 kg | |
| Generator power | 1 kW | |

The voltage amplitude characteristic with the position is shown in Fig 8. Moving part speed is 0.5 m/sec.

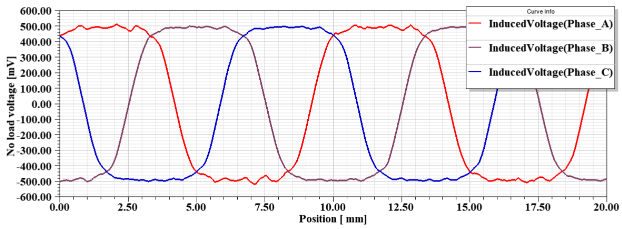


Fig. 8 No-load voltage versus position.

In Permanent Magnet (PM) electric linear generator the no-load voltage has a shape of a square (trapezoidal) waveform.

Given the current of each phase Fig.9, we studied the thrust force in the electric linear permanent magnet generator.

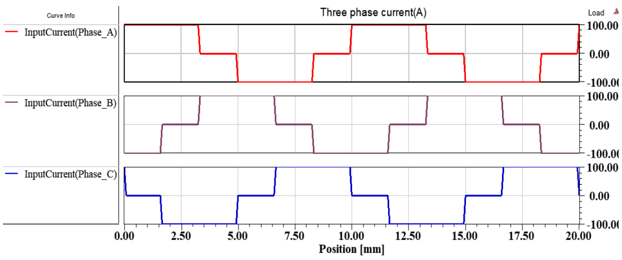


Fig. 9 Three-phase current versus position

Fig. 10 shows the thrust force versus displacement characteristic, which gives the relationship between the tangential force and displacement from the equilibrium position.

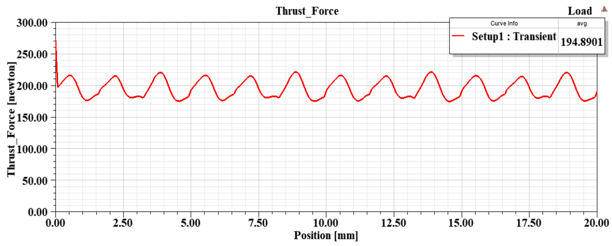


Fig. 10 Thrust force three-phase MALG versus displacement.

## 4. Conclusions

The Permanent Magnet Linear Generator Multi Air-gap Structure is designed and simulated using 2D FEM ANSYS Maxwell software. A prototype is being built at this time.

We investigated the effects of parameters including air-gap width, permanent magnet thickness, and slot opening width upon the cogging force. After analysis, the best parameters to decrease the cogging force were chosen.

## 5. References

[1] I., Boldea: 'Linear Electric Machines, Drives, and MAGLEVs Handbook', CRC Press, Taylor & Francis Group, 2013, 635 p.

[2] I., Boldea, and Syed A. Nasar: 'Linear Electric Actuator and Generator', Cambridge University Press, 1997, 237 p.

[3] J, Prudell, M, Stoddard, and all: 'A Permanent-Magnet Tubular Linear Generator for Ocean Wave Energy Conversion', IEEE Transactions on Industry Applications, Vol.48, NO.6, November- December 2010

[4] P.-E, Cavarec, and H.B, Ahmed and B, Multon: 'Force density improvements from increasing the number of airgap surfaces in synchronous linear actuators', Electric Power Applications, IEE Proceedings, 2003, 150, (1), pp. 106-116.

[5] D, Matt, and R, Goyet, and N, Haddad, and J, Lucidarme, and C, Rioux: 'Study of original structures of multi-airgap reluctance machines'. Proc. International Conference on Electrical Machines, Pise, Italy, 1988

[6] Young-shin Kwon, and Won-jong Kim: 'Detent-Force Minimization of Double-Sided Interior Permanent-Magnet Flat Linear Brushless Motor', IEEE Transactions on Magnetics, 0018-9464, 2015

[7] Eui-Jong Park, and Yong-Jae Kim: 'A Study on Reduction of End Cogging Force by Armature Offset Distance of Double-sided PMLSM', 9th International Conference on Power Electronics ECCE Asia, June 1-5, 2015

[8] M.W, Zouaghi, I, Abdennadher, and all: Prediction of Air Gap Flux Density Distribution of a T-LSM with Quasi-Halbach Magnetized PMs: Application of the cogging Force Minimization, 10th International Conference on Ecological vehicle and Renewable Energies, 2015

[9] G, Cipriani, V, Di Dio, and all: 'A Ferrite Tubular Linear Permanent Magnet Generator' (FTLPMG) analysis and design, 978-1-4799-4918-2/14, 2014

[10] Y, Huang, S, Zhou, and all: 'Design and Optimization for Unilateral Flat Permanent Linear Motor', 978-1-4673-0089-6/12, 2012

[11] J, Faiz, M, Ebrahimi-Salary, and all: Cogging Force Alleviation in Linear Permanent Magnet Generator, IEEE AFRICON 2009, 23-25 September 2009.